

2.1 INTRODUCTION

The successful operation of a catalytic process depends on the properties of the catalyst itself. These properties are a function of the synthesis method adopted. The challenge for the chemist, by the demands of catalytic processes, is to design and synthesize in high yield, novel catalysts, whose structures and properties can be predicted, varied and controlled, through eco-friendly routes. This is the challenge for the synthetic chemist by the demands of material technology.

Traditional ceramic processes use high temperatures. The present demands are making use of soft chemistry routes (low temperatures) which is popularly known as “*Chemie Douce*” by the French. Sol-gel method of synthesis is a soft chemistry route. Advantages of materials prepared by sol-gel synthesis is high homogeneity, high purity, low temperature processing, structural control of materials formed, materials with improved or desired properties and preparation of porous materials by use of templates. A great deal of interest has been shown in the application of sol-gel chemistry in various fields of technology. A majority of the materials prepared using the sol-gel method are ceramics, refractories and glasses. Attempts to apply the sol-gel technique for the preparation of catalysts is a relatively new venture, made since the last decade.

2.2 SOL-GEL PROCESS

Concepts and Terminologies

The sol-gel process is a wet-chemical technique for the fabrication of materials, employing low temperature, starting either from a chemical solution or colloidal particles (sol for solution or nanoscale particle) to produce an integrated network (gel). In general, sol-gel process can be regarded as the preparation of the sol, gelation of the sol and removal of the solvent. The overall sol-gel process can be represented by the following sequence of transformations [1]:



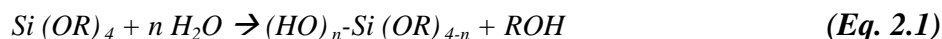
Precursors are starting materials, in which the essential basic entities for further network formation are present in the correct stoichiometry. Typical precursors are metal alkoxides and metal chlorides.

Sol is a colloidal suspension of particles in a liquid, the particles typically ranging from 1-100 nm in diameter. The solid particles in the colloidal phase are stable due to short-range forces such as Van der Waals attraction and surface charges.

Gel is a semi-rigid solid, in which solvent is contained in a network/framework of the material, which is either colloidal (essentially a concentrated sol) or polymeric. Gel is defined as a substance that contains a continuous solid skeleton enclosing a continuous liquid / fluid phases of colloidal dimensions.

In sol-gel processing, a sol of a given precursor is prepared, which involves the dissolution of the required metal ions either as alkoxides or other metallo-organic salts in a suitable solvent (alcohol) or as inorganic salts in water, which undergo hydrolysis, followed by condensation and polymerization reactions to produce highly condensed and branched network polymers, the gel. The networking depends on the functionality of the metal. Silicon with coordination number four, forms highly branched networks [2] (Figure 2.1a). In the gelation step, the fluid sol is transformed to a semirigid solid gel. Two types of gels are usually formed, colloidal and polymeric. Colloidal gels are formed from metal salt solutions, oxides and hydroxide sols, while polymeric gels are formed from metal alkoxide based sols. The name “sol-gel” is thus given to the process, because of the distinctive viscosity increase that occurs at a particular point in the sequence of steps. A sudden increase in viscosity is the common feature in sol-gel processing, indicating the onset of gel formation. Sol-gel process can be distinguished from precipitation by its specific property to stabilize a finely dispersed (mostly colloidal) phase in solution.

Typically, formation of a metal oxide via sol-gel route involves connecting the metal centers with oxo (M-O-M) or hydroxo (M-OH-M) bridges, generating metal-oxo or metal-hydroxo polymers in solution. The transformation of sol to gel takes place via hydrolysis and condensation reactions of the precursors. The hydrolysis reaction is represented taking silicon as an example:



In case of metal alkoxide precursors, R represents an alkyl group. The metal is totally hydrolyzed when $n = 4$. For any other value of n , partial hydrolysis takes place. In the condensation reaction, the two partially hydrolyzed molecules link together and liberate a small molecule such as H_2O or ROH . The general reaction is represented as:



The condensation takes place in such a way so as to maximize the number of M-O-M bonds and minimize terminal hydroxyl groups through internal condensation. Initially monomers add to form rings, creating 3-D structures. These compact structures are formed by leaving the hydroxyl groups outside, (Figure 2.1b) that serve as nuclei for further particle growth [3], that proceeds by Ostwald ripening mechanism, a process by which small particles precipitate on relatively larger insoluble particles, indicated by arrow heads in (Figure 2.1c). As particles grow in size the number of particles decrease. The polymerization behaviour of aqueous silica via sol-gel process at different pH is presented in (Figure 2.1d).

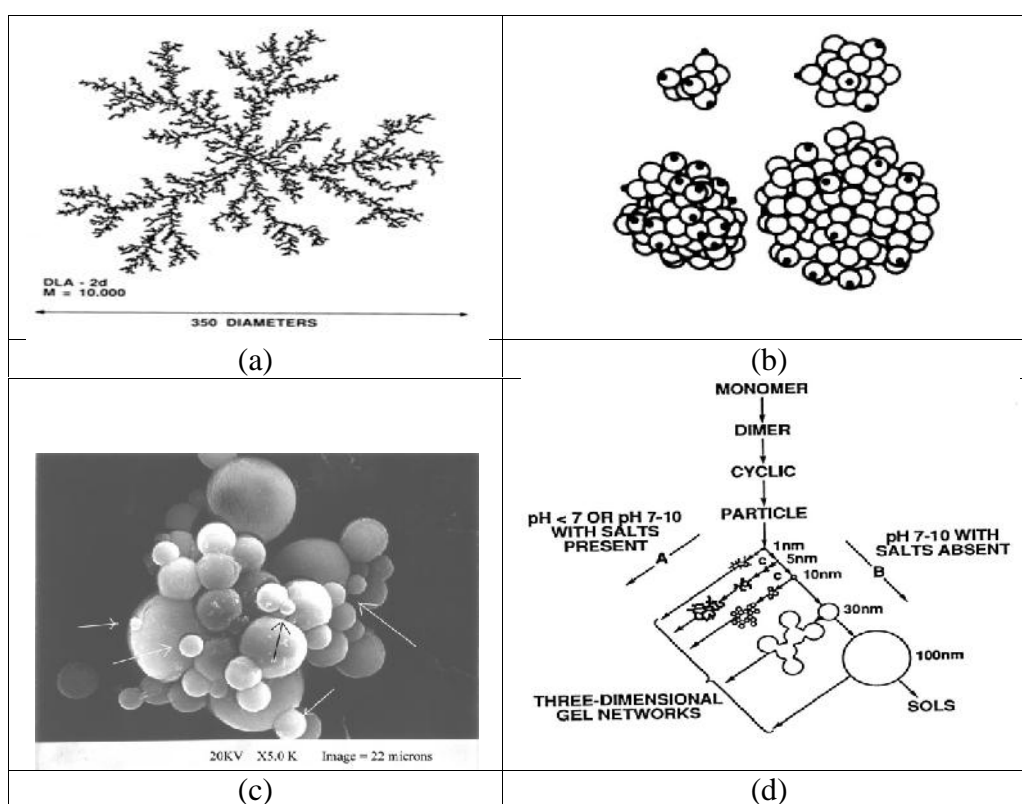


Figure 2.1 (a) Highly branched networks of silicon, (b) Condensation reactions leading to closed ring 3D structure, (c) SEM showing Ostwald ripening mechanism [3]. (d) Polymerization behavior of aqueous silica; A = in presence of salts / acidic medium, B = alkaline medium.

Sequential steps involved in sol-gel synthesis

Hydrolysis: It involves reaction of inorganic or organometallic precursor with water or a solvent, at ambient or slightly elevated temperature. Acid or base catalysts are added to speed up the reaction.

Polymerization: This step involves condensation of adjacent molecules wherein water/alcohol are eliminated and metal oxide linkages are formed. Polymeric networks grow to colloidal dimensions in the liquid (sol) state.

Gelation: It leads to the formation of a three dimensional network throughout the liquid, by the linking up of polymeric networks.

Ageing: A continuous change in structure and properties of a completely immersed gel in liquid is called ageing and represents the time between formation of the gel and removal of solvent. Aggregation of smaller polymeric units to the main network, progressively continues on ageing the gel. Solvent molecules however, remain inside the pores of the gel. Extensive ageing however, causes shrinkage of gel. Factors that affect ageing processes include temperature, time and pH of the pore liquid.

Drying: Here, solvent is removed at moderate temperatures (<200 °C) leaving the residue behind. During drying, the gel initially shrinks due to loss of pore fluid maintaining the liquid-vapour interface at the exterior surface of the gel. At the final stage of drying, liquid-vapour menisci recede into the gel interior [4]. The magnitude of the capillary pressure, P_c , exerted on the network, depends on the surface tension of the liquid, σ , the constant angle θ , and the pore size, r : given by $P_c = 2 \sigma \cos \theta / r$. If the pore size is very small, the capillary pressure will be large. The original gel network collapses due to this pressure [3]. Aging may be used to reduce the extent of collapse of the gel structure during drying. The resulting materials are identified based on drying conditions. Conventional evaporative drying such as heating a gel in an oven induces capillary pressure associated with the liquid-vapour interface within a pore, resulting in the collapse of the porous network. The sample thus obtained is called a **xerogel**, which has a relatively low surface area and pore volume. In supercritical drying, on the other hand, these deleterious effects are minimized due to differential capillary pressure and the resultant materials are known as **aerogels**. Consequently, they have high pore volumes, surface areas and low bulk densities. A third method of drying involves the freeze drying of the solvents at low temperature under reduced pressure. This method is similar to the lyophilization technique adopted in pharmaceutical industries and the product is called **cryogel**. Another method of drying is subjecting the gel to ultrasonic vibration at room temperature to remove the solvent. The gel thus obtained is called a **sonogel**.

Dehydration: This step is carried out between 400°C and 800°C to drive off the organic residues and chemically bound water. A thermal treatment firing/calcination may be performed in order to favour further polycondensation and enhanced mechanical property, when following changes, such as loss of solvents, pyrolysis of the organics, structural rearrangement and densification or crystallization are observed.

Densification: Heating the porous gel at high temperatures, leads to formation of a dense oxide product. The densification temperature depends considerably on the dimensions of the pore network, the connectivity of the pores, and surface area.

Sequential steps involved in sol-gel process is presented in Figure 2.2

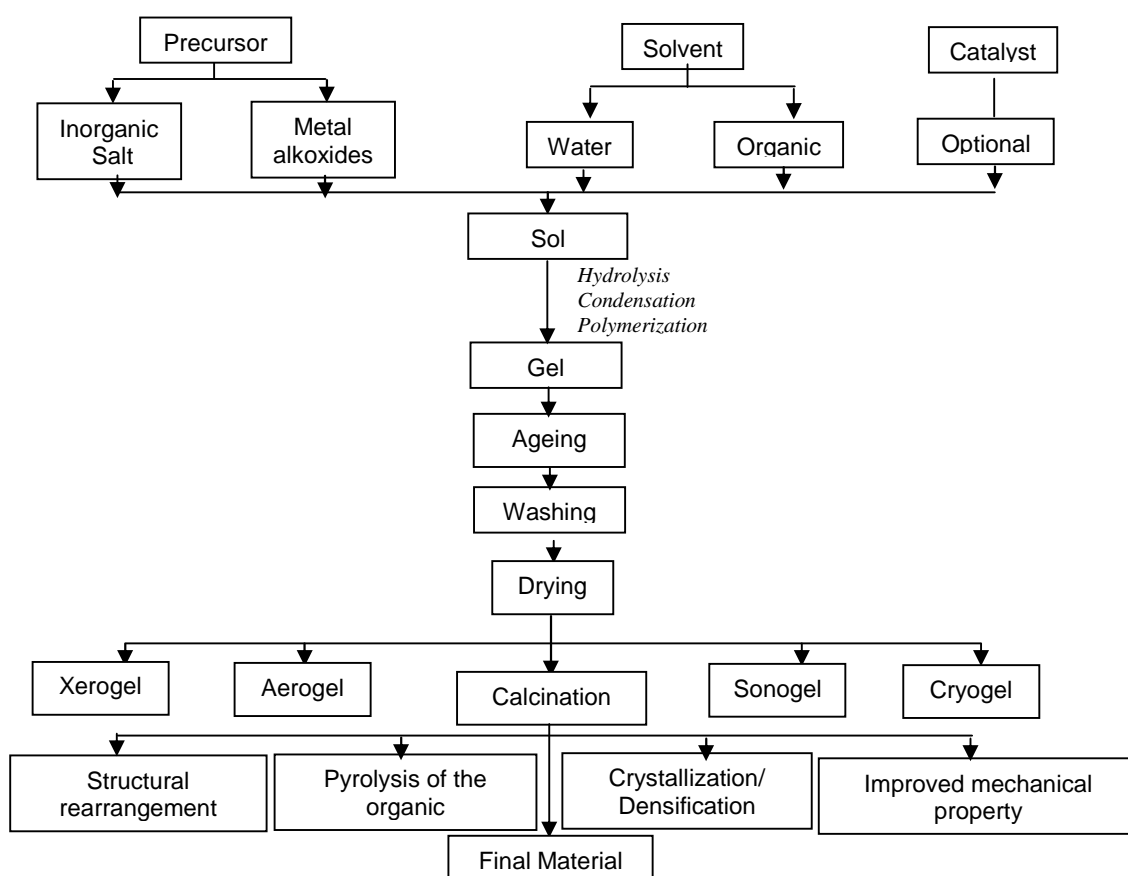


Figure 2.2 Sequential steps involved in sol-gel process

Conditions for sol-gel synthesis

It is possible to tailor specific properties in a material by tuning the various conditions of the sol-gel process, outlined as follows:

pH of the hydrolysis: The pH during hydrolysis mainly decides the nature of the pores, surface area and density of the materials. In general, acid catalyzed hydrolysis gives a microporous network, while base catalyzed hydrolysis leads to the formation

of a mesoporous network. The preparation of micro or mesoporous materials in a neutral medium has been reported [5].

Rate of addition of water: The rate of addition of water during the preparation of the sol affects the rate of hydrolysis and condensation which in turn influence the texture and morphology of the gel.

Temperature of gelation: The rate of gelation depends on the temperature at which the sol is aged or heated for the removal of the solvent or for the facilitation of hydrolysis. If the temperature is lower, the rate of hydrolysis is slower and the particle size is relatively smaller. This results in reduced pore collapse and yields a well defined porous network.

Aging of Gels: Aging is the process of keeping the gels in various solutions for a period of time in order to increase the strength of the gel network, so that cracking of gels during drying can be prevented. The chemical reactions that cause gelation, continue long after gel point strengthening, stiffening and shrinkage of the network [4,6]. The composition, structure and properties of gel change during aging. The changes that occur during aging are categorized as,

- Polymerization: Increase in connectivity of the gel network by condensation reactions.
- Coarsening: Process of dissolution and reprecipitation driven by differences in solubility between surfaces with different radii of curvature.
- Syneresis: Shrinkage of the gel and the resulting expulsion of liquid from the pores.

Drying control chemical agents (DCCAs): The presence of DCCAs has a significant influence on the particle texture and morphology. Various DCCAs useful in controlling the porosity and bulk density are formamide, glycerol and oxalic acid.

Calcination temperature: the calcination temperature is also important in controlling the pore size and density of the materials.

Conclusions, Advantages and Disadvantages of Sol-Gel process

The sol-gel method, thus offers the possibility to prepare solids with pre-determined structure, by varying the experimental conditions such as the choice of reagents, concentration, mode and rate of mixing, temperature, pH, ageing and drying conditions. Variation in any of these parameters yields materials with different characteristics. The preparation procedure thus affects the composition and structure,

which is further reflected in the properties/performance such as porosity, surface polarity and crystallinity. The various steps involved in the sol-gel technique described above may or may not be followed. In practice, however, a modified sol-gel route is followed.

Advantages of sol-gel process include increased homogeneity, high purity, low processing temperature and high surface area of the gels or powders obtained. The inherent usefulness of this approach is largely due to the ease with which sol-gel derived materials can be prepared, modified, and processed. The mild reaction conditions afford an opportunity to incorporate various organic moieties into inorganic compounds. Furthermore, the average pore size, pore size distribution, surface area, refractive index and polarity of the resultant matrix can also be controlled and tailored by manipulations in the sol-gel processing conditions. Disadvantages of the sol-gel process include, large shrinkage during processing, creation of fine pores, presence of hydroxyl groups when hydroxides are used, residual carbon in final material originating from templates, health hazards of organic solvents, and finally long processing times.

The present chapter deals with synthesis and characterization of solid acid catalysts (SACs) possessing inherent and induced acidity.

Type – I catalysts M(IV)PWs [where, M(IV)=Zr,Sn,Ti] of the class of TMBA salts possessing inherent acidity -

- Zirconium (IV) Phosphotungstate (ZrPW),
- Titanium (IV) Phosphotungstate (TiPW),
- Tin (IV) Phosphotungstate (SnPW),

have been synthesized by sol-gel route.

Type – II catalysts 12-TPA/M(IV)O₂ [where, M(IV)=Zr,Sn,Ti] possessing induced acidity -

- 12-TPA/ZrO₂,
- 12-TPA/TiO₂,
- 12-TPA/SnO₂,

have been synthesized by process of anchoring and calcination.

2.3 EXPERIMENTAL

Materials

Zirconium oxychloride ($\text{ZrOCl}_2 \cdot 8\text{H}_2\text{O}$), Titanium tetrachloride (TiCl_4) and Stannic tetrachloride (anhydrous SnCl_4) were procured from Loba chemicals. Sodium dihydrogen phosphate ($\text{NaH}_2\text{PO}_4 \cdot 2\text{H}_2\text{O}$) and Sodium tungstate ($\text{Na}_2\text{WO}_4 \cdot 2\text{H}_2\text{O}$) were obtained from Merck, India. H_2SO_4 , HNO_3 , HCl , NaOH , KOH and organic solvents used were of analytical grade procured from Loba Chemicals, Mumbai. Deionized water (DIW) was used for all the studies.

Synthesis of M(IV) Phosphotungstates [M(IV)PWs] (Type-I Catalysts)

M(IV)PWs were synthesized by sol-gel method, the main objective being to obtain a material with high cation exchange capacity (CEC)/protonating ability, varying several parameters such as mole ratio of reactants, temperature, mode of mixing (metal salt solution to anion salt solution or vice versa) and rate of mixing. Several sets of materials were prepared varying conditions in each case using CEC as the indicative tool. The optimized parameters for synthesis of ZrPW, TiPW and SnPW have been presented in tables 2.1 to 2.3 respectively.

Synthesis of ZrPW (at optimized condition)

An aqueous solution mixture of $\text{NaH}_2\text{PO}_4 \cdot 2\text{H}_2\text{O}$ (0.1M, 50ml) and $\text{Na}_2\text{WO}_4 \cdot 2\text{H}_2\text{O}$ (0.1M, 50ml) was added dropwise (flow rate $1 \text{ ml} \cdot \text{min}^{-1}$) to an aqueous solution of $\text{ZrOCl}_2 \cdot 8\text{H}_2\text{O}$ (0.2M, 50ml) with continuous stirring for an hour at 70°C . The gelatinous precipitates obtained was filtered, washed with DIW and dried at room temperature. The material was then broken down to the desired particle size (30-60 mesh) by grinding and sieving (Step - I).

Synthesis of TiPW (at optimized condition)

An aqueous solution mixture of $\text{NaH}_2\text{PO}_4 \cdot 2\text{H}_2\text{O}$ (0.1M, 50ml) and $\text{Na}_2\text{WO}_4 \cdot 2\text{H}_2\text{O}$ (0.1M, 50ml) was added dropwise (flow rate $1 \text{ ml} \cdot \text{min}^{-1}$) to a solution of TiCl_4 (0.2M, 50ml, prepared in 10% W/V H_2SO_4 solution) with continuous stirring for an hour at room temperature. The gelatinous precipitates obtained was aged for 1h, then filtered and washed with DIW followed by drying at room temperature. The material was then broken down to the desired particle size (30-60 mesh) by grinding and sieving (Step - I).

Synthesis of SnPW (at optimized condition)

An aqueous solution mixture of NaH₂PO₄·2H₂O (0.1M, 50ml) and Na₂WO₄·2H₂O (0.1M, 50ml) was added dropwise (flow rate 1 ml·min⁻¹) to a solution of SnCl₄ (0.1M, 100ml, prepared in 0.1M HCl) with continuous stirring for an hour at room temperature. The gelatinous precipitates obtained was aged for 3h, then filtered and washed with DIW followed by drying at room temperature. The material was then broken down to the desired particle size (30-60 mesh) by grinding and sieving (Step - D).

Acid treatment

5 g of material (ZrPW/TiPW/SnPW) prepared above in step – I, was treated with 50 mL of 1 M HNO₃ for 30 min with occasional shaking. The material was then separated from acid by decantation and treated with deionized water to remove adhering acid. This process (acid treatment) was repeated at least 5 times. After final washing, the material was dried at room temperature. These materials were used for all studies.

Table 2.1 Optimization of parameters for synthesis of ZrPW.

| Parameters optimized | No. | Concentration (M) | | | Volume (ml) | | | Mole ratio Zr:P:W | Temp. (°C) | Stirring time (h) | Aging time (h) | CEC meq/g |
|----------------------|------------|-------------------|------------|------------|-------------|-----------|-----------|-------------------|------------|-------------------|----------------|-------------|
| | | Zr | P | W | Zr | P | W | | | | | |
| Concentration | 1 | 0.1 | 0.1 | 0.1 | 50 | 50 | 50 | 1:1:1 | 30 | 1 | 15 | 0.56 |
| | 2 | 0.2 | 0.1 | 0.1 | 50 | 50 | 50 | 2:1:1 | 30 | 1 | 15 | 0.98 |
| | 3 | 0.2 | 0.1 | 0.2 | 50 | 50 | 50 | 2:1:2 | 30 | 1 | 15 | 0.44 |
| | 4 | 0.2 | 0.2 | 0.1 | 50 | 50 | 50 | 2:2:1 | 30 | 1 | 15 | 0.89 |
| | 5 | 0.1 | 0.2 | 0.2 | 50 | 50 | 50 | 1:2:2 | 30 | 1 | 15 | 0.38 |
| Volume | 6 | 0.1 | 0.1 | 0.1 | 100 | 50 | 50 | 2:1:1 | 30 | 1 | 15 | 1.08 |
| | 7 | 0.2 | 0.1 | 0.1 | 100 | 50 | 50 | 4:1:1 | 30 | 1 | 15 | 0.75 |
| Aging Time | 8 | 0.2 | 0.1 | 0.1 | 50 | 50 | 50 | 2:1:1 | 30 | 1 | 1 | 0.90 |
| | 9 | 0.2 | 0.1 | 0.1 | 50 | 50 | 50 | 2:1:1 | 30 | 1 | 3 | 0.92 |
| | 10 | 0.2 | 0.1 | 0.1 | 50 | 50 | 50 | 2:1:1 | 30 | 1 | 5 | 0.92 |
| Temperature | 11* | 0.2 | 0.1 | 0.1 | 50 | 50 | 50 | 2:1:1 | 70 | 1 | 0 | 1.20 |
| Stirring Time | 12 | 0.2 | 0.1 | 0.1 | 50 | 50 | 50 | 2:1:1 | 70 | 2 | 0 | 1.18 |

(* Optimum condition for synthesis of ZrPW)

Table 2.2 Optimization of parameters for synthesis of TiPW.

| Parameters optimized | No. | Concentration (M) | | | Volume (ml) | | | Mole ratio | Temp. °C | Stirring time (h) | Aging time (h) | CEC meq/g |
|----------------------|-----------|-------------------|------------|------------|-------------|-----------|-----------|--------------|-----------|-------------------|----------------|-------------|
| | | Ti | P | W | Ti | P | W | Ti:P:W | | | | |
| Concentration | 1 | 0.1 | 0.1 | 0.1 | 50 | 50 | 50 | 1:1:1 | 30 | 1 | 15 | 3.06 |
| | 2 | 0.2 | 0.1 | 0.1 | 50 | 50 | 50 | 2:1:1 | 30 | 1 | 15 | 3.18 |
| | 3 | 0.2 | 0.1 | 0.2 | 50 | 50 | 50 | 2:1:2 | 30 | 1 | 15 | 2.27 |
| | 4 | 0.2 | 0.2 | 0.1 | 50 | 50 | 50 | 2:2:1 | 30 | 1 | 15 | 3.16 |
| | 5 | 0.1 | 0.2 | 0.2 | 50 | 50 | 50 | 1:2:2 | 30 | 1 | 15 | 2.60 |
| Volume | 6 | 0.1 | 0.1 | 0.1 | 100 | 50 | 50 | 2:1:1 | 30 | 1 | 15 | 3.45 |
| | 7 | 0.2 | 0.1 | 0.1 | 100 | 50 | 50 | 4:1:1 | 30 | 1 | 15 | 2.91 |
| Aging Time | 8* | 0.2 | 0.1 | 0.1 | 50 | 50 | 50 | 2:1:1 | 30 | 1 | 1 | 3.48 |
| | 9 | 0.2 | 0.1 | 0.1 | 50 | 50 | 50 | 2:1:1 | 30 | 1 | 3 | 2.42 |
| | 10 | 0.2 | 0.1 | 0.1 | 50 | 50 | 50 | 2:1:1 | 30 | 1 | 5 | 2.75 |
| Temperature | 11 | 0.2 | 0.1 | 0.1 | 50 | 50 | 50 | 2:1:1 | 70 | 1 | 0 | 2.77 |
| Stirring Time | 12 | 0.2 | 0.1 | 0.1 | 50 | 50 | 50 | 2:1:1 | 70 | 2 | 1 | 3.28 |

(* Optimum condition for synthesis of TiPW)

Table 2.3 Optimization of parameters for synthesis of SnPW.

| Parameters optimized | No | Concentration (M) | | | Volume (ml) | | | Mole ratio | Temp. °C | Stirring time (h) | Aging time (h) | CEC meq/g |
|----------------------|-----------|-------------------|------------|------------|-------------|-----------|-----------|--------------|-----------|-------------------|----------------|-------------|
| | | Sn | P | W | Sn | P | W | Sn:P:W | | | | |
| Concentration | 1 | 0.1 | 0.1 | 0.1 | 50 | 50 | 50 | 1:1:1 | 30 | 1 | 15 | 1.93 |
| | 2 | 0.2 | 0.1 | 0.1 | 50 | 50 | 50 | 2:1:1 | 30 | 1 | 15 | 1.65 |
| | 3 | 0.2 | 0.1 | 0.2 | 50 | 50 | 50 | 2:1:2 | 30 | 1 | 15 | 1.40 |
| | 4 | 0.2 | 0.2 | 0.1 | 50 | 50 | 50 | 2:2:1 | 30 | 1 | 15 | 1.76 |
| | 5 | 0.1 | 0.2 | 0.2 | 50 | 50 | 50 | 1:2:2 | 30 | 1 | 15 | 1.83 |
| Volume | 6 | 0.1 | 0.1 | 0.1 | 100 | 50 | 50 | 2:1:1 | 30 | 1 | 15 | 1.99 |
| | 7 | 0.2 | 0.1 | 0.1 | 100 | 50 | 50 | 4:1:1 | 30 | 1 | 15 | 1.82 |
| Aging Time | 8 | 0.1 | 0.1 | 0.1 | 100 | 50 | 50 | 2:1:1 | 30 | 1 | 1 | 2.19 |
| | 9* | 0.1 | 0.1 | 0.1 | 100 | 50 | 50 | 2:1:1 | 30 | 1 | 3 | 2.44 |
| | 10 | 0.1 | 0.1 | 0.1 | 100 | 50 | 50 | 2:1:1 | 30 | 1 | 5 | 2.30 |
| Temperature | 11 | 0.1 | 0.1 | 0.1 | 100 | 50 | 50 | 2:1:1 | 70 | 1 | 0 | 2.23 |
| Stirring Time | 12 | 0.1 | 0.1 | 0.1 | 100 | 50 | 50 | 2:1:1 | 30 | 2 | 1 | 2.38 |

(*Optimum condition for synthesis of SnPW)

Synthesis of 12-TPA supported Oxides (12-TPA/ZrO₂, 12-TPA/TiO₂, 12-TPA/SnO₂) (Type-II Catalysts)

For preparation of ZrO₂, TiO₂ and SnO₂, aqueous solutions of ZrOCl₂.8H₂O (0.3M, 100 ml), TiCl₄ (0.9M, 100 ml) and SnCl₄.5H₂O (0.3M, 100 ml) were prepared

to which liq. NH_3 (25%) was added dropwise with vigorous stirring. The pH of the solutions was adjusted to 9.5. In all the cases, precipitates obtained were filtered and washed with DIW till removal of adhering ions and then dried at 120°C for 3 h followed by calcination at 550°C for 5h.

For the preparation of 12-TPA supported catalysts, a series of aqueous solutions containing 10-30 wt % of 12-TPA per gram of precalcined oxides were used, and the mixture was stirred for 36 h. The excess water was removed at 70°C under vacuum. The resulting solid was dried at 120°C for 3h, followed by grinding to get a fine powder (600 mesh) [7]. In each case surface acidity was used as the indicative tool. The optimization of wt. % loading of 12-TPA onto oxides have been presented in Table 2.4. Amongst the different wt. % of 12-TPA loaded, 20 wt. % loading of 12-TPA onto oxides gives maximum surface acidity. Thus, for all studies 20 wt.% 12-TPA/M(IV) O_2 have been used and abbreviated as 12-TPA/M(IV) O_2 -20, where M(IV) = Zr, Ti and Sn.

Table 2.4 Optimization of loading of 12-TPA (wt. %) onto M(IV) O_2 .

| Materials | Surface Acidity (mmol/g) (at 700°C preheating temperature) |
|--|---|
| 10 wt. % 12-TPA/ ZrO_2 | 0.113 |
| 20 wt. % 12-TPA/ZrO_2 | 0.170 |
| 30 wt. % 12-TPA/ ZrO_2 | 0.121 |
| 10 wt. % 12-TPA/ TiO_2 | 0.195 |
| 20 wt. % 12-TPA/TiO_2 | 0.270 |
| 30 wt. % 12-TPA/ TiO_2 | 0.214 |
| 10 wt. % 12-TPA/ SnO_2 | 0.150 |
| 20 wt. % 12-TPA/SnO_2 | 0.220 |
| 30 wt. % 12-TPA/ SnO_2 | 0.201 |

2.4 MATERIAL CHARACTERIZATION

The synthesized materials have been subjected to **instrumental methods of characterization** and **catalyst characterization**. Chemical stability of all the synthesized materials has been assessed in various media (e.g. acids, bases and organic solvents etc) and in the media/environment where catalyst would operate. This gives us an idea about the stability/resistivity of the material in these environments. Further, the protonating ability [in terms of cation exchange capacity (CEC)] has been determined for M(IV)PWs (Type – I catalysts).

Instrumental Methods of Characterization

The instrumental methods of analysis include elemental analysis (ICP-AES), spectral analysis (FTIR), thermal analysis (TGA), X-ray diffraction (XRD) studies and scanning electron microscopy (SEM).

Fourier Transform Infrared Spectroscopy (FTIR)

In the present study, the FTIR spectra of the synthesized materials were recorded to confirm the presence of structural hydroxyl groups in the material. FTIR spectrum of each material was obtained using KBr pellet on Shimadzu (Model 8400S).

The FTIR spectra for all the materials are presented in figures 2.3 (a) - 2.8 (a). FTIR spectrum of M(IV)PWs (Type-I catalysts) exhibits broad band in the region $\sim 3400\text{ cm}^{-1}$ which is attributed to asymmetric and symmetric -OH stretching vibration due to residual water and presence of structural hydroxyl groups, H^+ of the -OH being Brønsted acid sites in nature. These bands indicate the presence of structural hydroxyl groups/catalytic sites in the materials. These sites are also referred to as defective P-OH groups [8]. A sharp medium band at $\sim 1635\text{ cm}^{-1}$ is attributed to aquo H-O-H bending. A band in the region $\sim 1083\text{ cm}^{-1}$ is attributed to the presence of P=O stretching in all samples.

FTIR spectrum of 12-TPA/ ZrO_2 -20, 12-TPA/ TiO_2 -20 and 12-TPA/ SnO_2 -20 (Type-II catalysts) exhibits peaks at $\sim 3450\text{ cm}^{-1}$, $\sim 1635\text{ cm}^{-1}$, $\sim 1083\text{ cm}^{-1}$, $\sim 987\text{ cm}^{-1}$, which corresponds to asymmetric and symmetric -OH stretching, P-O-H bending, P=O stretching and W-O stretching, respectively.

Thermal analysis

Thermal analysis (TGA) was performed on a Shimadzu (Model TGA 50) thermal analyzer at a heating rate of $10^\circ\text{C}\cdot\text{min}^{-1}$.

Thermograms obtained for all the materials are presented in figures 2.3 (b) - 2.8 (b). TGA of M(IV)PWs (Type-I catalysts) shows weight loss in the temperature range of 40°C - 150°C to be $\sim 20\%$ (ZrPW), $\sim 21\%$ (TiPW) and $\sim 15\%$ (SnPW), which corresponds to loss of surface moisture and hydrated water. Weight loss in the temperature range of 150°C - 650°C is found to be $\sim 7\%$ (ZrPW), $\sim 4\%$ (TiPW) and $\sim 6\%$ (SnPW), which is probably due to the condensation of structural hydroxyl groups [9,10].

TGA thermograms of 12-TPA/ZrO₂-20, 12-TPA/TiO₂-20 and 12-TPA/SnO₂-20 (Type-II catalysts) exhibit 0.9%, 0.4% and 1.4% weight loss respectively, in the temperature range of 30°C - 150°C which corresponds to the loss of surface moisture. Thereafter in the region 200°C - 600°C there is a negligible weight loss which indicates fairly stable nature of the materials.

X-ray diffraction studies

X-ray diffractogram ($2\theta = 10 - 80^\circ$) was obtained on X-ray diffractometer (Bruker AXS D8) with Cu-K radiation with nickel filter. Absence of sharp peaks in X-ray diffractogram of M(IV)PWs [Figures 2.3 (c) – 2.5 (c)] reveals the amorphous nature of M(IV)PWs.

X-ray diffractogram of pure 12-TPA has been presented in Figures 2.6 (c) - 2.8 (c). X-ray diffractogram of 12-TPA/ZrO₂-20 [Figure 2.6 (d)] shows intense and well defined characteristic diffraction peaks at 2θ values of 31.4, 35.2, 50.1, and 59.9 (JCPDS data card no. 17-923). X-ray diffractogram pattern of 12-TPA/TiO₂-20 [Figure 2.7 (d)] shows characteristic diffraction peaks at 2θ values of 25.2, 37.8, 48.0, 53.8, 55.0, 62.1 and 75.0 correspond to the crystal planes of (101), (004), (200), (105), (211), (213) and (215) respectively, indicates formation of anatase TiO₂ (JCPDS data card no. 21-1272). X-ray diffractogram pattern of 12-TPA/SnO₂-20 shows [Figure 2.8 (d)] characteristic diffraction peaks at 2θ values of 26.5, 33.8 and 51.8 correspond to the crystal planes of (110), (101) and (211) respectively, indicates formation tetragonal SnO₂ (JCPDS data card no. 41-1445).

Scanning electron microscopy (SEM)

SEM was scanned on Jeol JSM-5610-SLV scanning electron microscope. SEM images of Type – I catalysts [M(IV)PWs] are presented in figures 2.3(d) - 2.5(d) while that of Type – II catalysts [12-TPA/M(IV)O₂-20] are presented in figures 2.6(f) - 2.8(f). SEM images of ZrO₂, TiO₂ and SnO₂ are presented in figures 2.6(e) - 2.8(e). It is observed that, all the synthesized catalysts exhibit irregular morphology.

Formulation of synthesized compounds based on elemental analysis

In the present study, elemental analysis was performed on ICP-AES spectrometer (Labtam, 8440 Plasmalab). The concentration of different elements measured at ppm level, is converted into the % weight of the element, by incorporating the dilution factor. These values are then converted into moles of each

element. Elemental analysis performed by ICP-AES for M(IV)PWs (Type-I catalysts) and 12-TPA/M(IV)O₂-20 (Type-II catalysts) has been presented in Tables 2.5-2.10.

In formulating the composition of M(IV)PWs, it is assumed that the hydroxyl protons are lost, to coordinate with the tetravalent metal, forming M-O-P or M-O-W bonds. Formulation is thus based on metal : phosphorous : tungsten ratio. Elemental analysis shows that the mole ratio of M(IV):P:W in M(IV)PWs (Type – I catalysts) to be 2:1:1. Based on the elemental analysis (ICP-AES) and TGA data, ZrPW, TiPW and SnPW are formulated as ZrH₃PWO₉·9H₂O, TiH₃PWO₈·7H₂O and SnH₃PWO₈·7H₂O respectively. The number of water molecules in each case is calculated using Alberti and Torracca (1968) formula [11].

For 12-TPA/M(IV)O₂-20 (Type – II catalysts) the amount of 12-TPA loaded on M(IV)O₂ is observed to be ~20 wt. % (Tables 2.8 – 2.10).

Catalyst characterization

Surface area determination (BET method)

Adsorption desorption isotherms of Nitrogen (N₂) was recorded by BET (Braunauer Emmett Teller) multipoint method using a Micromeretics Gemini 2220 series surface area analyzer, at -196 °C after degassing the sample at 300 °C for 4 h. Surface area values determined (by BET method) and pore diameter for all materials have been presented in table 2.5 – 2.10.

Protonating ability / Cation exchange capacity (CEC)

The cation exchange capacity (CEC) reflects on the protonating ability and thus the acidity of the materials. The term CEC is intended to describe the total available exchange capacity of an ion exchanger, as described by the number of functional groups on it. This value is constant for a given ion exchange material and is expressed in milli equivalents per gram (meq.g⁻¹), based on dry weight of material in given form (such as H⁺).

In the present study, Na⁺-CEC of M(IV)PWs (Type – I catalysts) were determined by the column method at optimized volume and concentration of sodium acetate solution [9,10]. Firstly, a fixed volume (250 mL) of sodium acetate solution of varying concentration (0.1 M, 0.2 M, 0.3 M, 0.4 M, 0.5 M, 0.6 M, 0.7 M) was passed through a glass column (30 cm × 1 cm internal diameter) containing 0.5 g of the exchanger say ZrPW, maintaining a flow rate of 0.5 mL·min⁻¹ and effluent (containing H⁺ ions eluted out) titrated against 0.1 M NaOH solution. The optimum

concentration of eluent is thus determined. Now, eluent of optimum concentration was used and 10 mL fractions passed through the column maintaining a flow rate 0.5 mL·min⁻¹. This experiment was conducted to find out the minimum volume necessary for a complete elution of the H⁺ ions, which reflects the efficiency of the column. Using these optimized parameters Na⁺ CEC was determined, using the formula aV/W , where a is molarity, V the amount of alkali used during titration, and W is the weight of the exchanger.

The CEC values for Type-I catalysts [M(IV)PWs] are presented in tables 2.5-2.7. The effect of calcination on CEC was studied using 1 g of each sample, calcined at the temperatures 150°C, 200°C and 700°C for 2 h, cooled to room temperature and CEC determined by the column method [9,10] (Tables 2.5-2.7). It is observed that, CEC values decrease with increase in calcination temperature probably due to condensation of structural hydroxyl groups. This is well supported by TGA and FTIR spectra of the calcined samples, where the intensity of the peak at ~ 3400 cm⁻¹ and ~ 1620 cm⁻¹ representative of the –OH group diminishes as calcination temperature increases [Figures 2.3 (a) - 2.5 (a)].

Surface acidity determination (NH₃-TPD method)

Surface acidity was determined on Micromeritics Chemisorb 2720, by a temperature programmed desorption (TPD) of ammonia. All the synthesized materials were preheated at 150°C, 200°C and 700°C. Ammonia was chemisorbed at 120°C and then desorption was carried out upto 700°C at a heating rate of 10°C/min in all cases.

Surface acidity determined by NH₃-TPD at 150°C, 200°C and 700°C preheating temperatures are presented in tables 2.5-2.10. M(IV)PWs (Type-I catalysts) exhibit broad desorption peaks [Figures 2.3 (e) - 2.5 (e)] compared to 12-TPA/M(IV)O₂-20 (Type-II catalysts) [Figures 2.6(g) - 2.8(g)], which is in accordance with the amorphous and crystalline nature of the materials respectively [12]. Acidity in the M(IV)PWs is due to the presence of structural hydroxyl protons, H⁺ of the –OH being the Bronsted acid sites. Further, surface acidity values of M(IV)PWs depend on the size and charge of the cation. Smaller size and higher charge of the cation indicates greater tendency to release a proton, i.e. H⁺ of the –OH groups present in M(IV)PWs. In the present study Zr⁴⁺, Ti⁴⁺ and Sn⁴⁺, all metal ions being tetravalent as well as bearing common anion PO₄³⁻ and WO₄²⁻, size of the cation (Zr⁴⁺-0.86 Å, Ti⁴⁺-0.74 Å, Sn⁴⁺-0.83 Å) seems to play a dominant role [12]. Thus the acidity

in the M(IV)PWs (Type-I catalysts) follows the order $\text{TiPW} > \text{SnPW} > \text{ZrPW}$. Decrease in surface acidity for M(IV)PWs with increasing preheating temperatures could be attributed to condensation of structural hydroxyl groups as discussed above in thermal behavior of these materials [8,9]. This is well supported by CEC values, which reflect on the protonating ability and thus the acidity of the materials. CEC values also decrease with increasing calcination/preheating temperature have already been discussed in FTIR spectra of calcined samples.

Chemical resistivity

Chemical resistivity/stability in various media - acids (varying concentration of H_2SO_4 , HNO_3 , HCl), bases (varying concentration of NaOH and KOH) and organic reagents/solvents (ethanol, propanol, butanol, benzyl alcohol, 2-ethyl 1-hexanol, benzene, acetone, cyclohexane, toluene, xylene, benzyl chloride, acetyl chloride, anisole, veratrole, acetic acid, benzaldehyde, cyclohexanone, acetophenone and nitrobenzene) was studied by taking 500 mg of the material in 50 mL of the particular medium and allowing to stand for 24 h. The change in colour, nature, weight as well as solubility was observed. Further, to confirm the stability/solubility of the material in particular media, supernatant liquid was checked qualitatively for respective elements of the material.

Maximum tolerable limits in a particular medium evaluated have been presented in tables 2.5-2.10. In general, all the materials are stable in acid and organic solvent media but not so stable in base medium.

Table 2.5 Characterization of ZrPW

| Appearance | | White hard granules | | | |
|---|-----------------------------|--|-----------------------|------------------------|-----------------------|
| Cation exchange capacity (CEC)/Protonating ability | Temperature (°C) | CEC (meq.g ⁻¹) | | | |
| | RT | 1.20 | | | |
| | 150 | 0.98 | | | |
| | 200 | 0.76 | | | |
| Chemical Stability (Maximum tolerable limits) | Acids | 18N H ₂ SO ₄ , 16N HNO ₃ , 11.3N HCl | | | |
| | Bases | 5 N NaOH, 5 N KOH | | | |
| | Organic reagents | Ethanol, propanol, butanol, benzyl alcohol, 2-ethyl-1-hexanol, acetone, cyclohexane, toluene, xylene, benzyl chloride, acetyl chloride, anisole, veratrole, methyl acetoacetate, acetic acid benzaldehyde, cyclohexanone, acetophenone and nitrobenzene. | | | |
| Instrumental Methods of Analysis | | | | | |
| Elemental Analysis | Technique/Method | Elements | | | |
| | | Zr | P | W | |
| | ICP-AES (%) | 26.88 | 4.96 | 25.37 | |
| FTIR | Peaks (cm ⁻¹) | ~3400 cm ⁻¹ | ~1635cm ⁻¹ | ~1083 cm ⁻¹ | ~525 cm ⁻¹ |
| | Groups assigned | O-H _{str} | H-O-H _{ben} | P=O _{str} | W-O-P _{str} |
| TGA | Temperature range (°C) | 40-150 | | | |
| | % Weight loss | 19.78% (loss of surface moisture) | | | |
| | Temperature range (°C) | 150-650 | | | |
| | % Weight loss | 7.25 % (condensation of pendant -OH groups) | | | |
| XRD | Nature of material | Amorphous | | | |
| SEM | Size of particles | Irregular | | | |
| Catalyst characterization | | | | | |
| Surface area (by BET method) | | 80.96 m ² /g | | | |
| Average Pore diameter (nm) | | 2.05 | | | |
| Pore Volume (mL·g⁻¹) | | 0.04 | | | |
| Surface acidity (by NH₃-TPD method) | Preheating temperature (°C) | | Acidity (mmol/g) | | |
| | 150°C | | 9.34 | | |
| | 200°C | | 6.05 | | |
| | 700°C | | 3.90 | | |

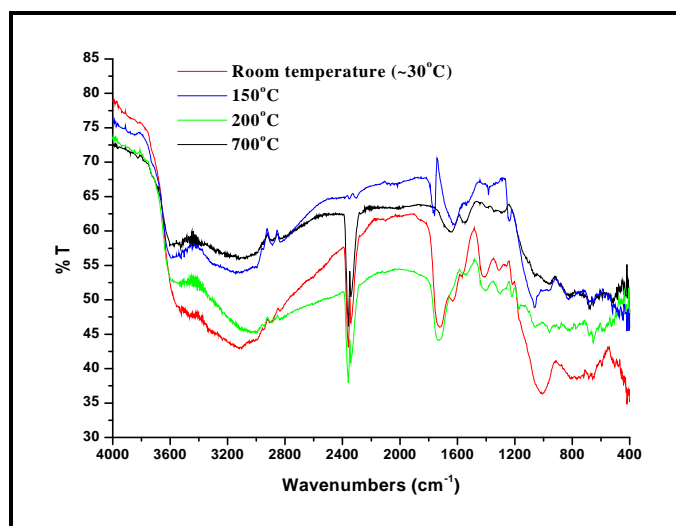


Figure 2.3 (a) FTIR spectra of ZrPW

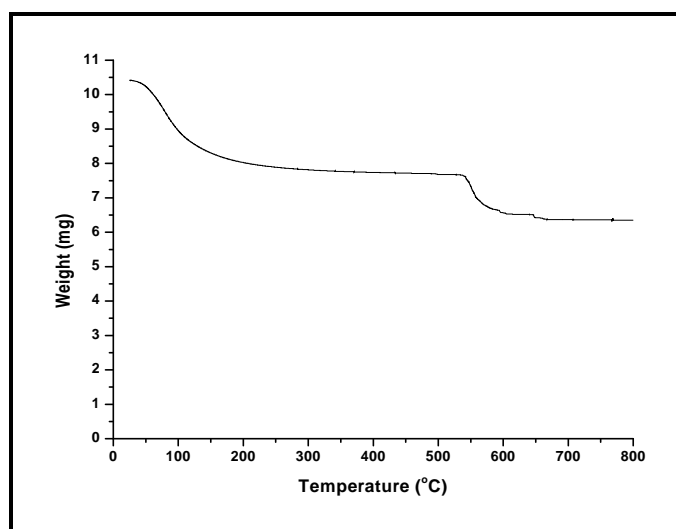


Figure 2.3 (b) TGA plot of ZrPW

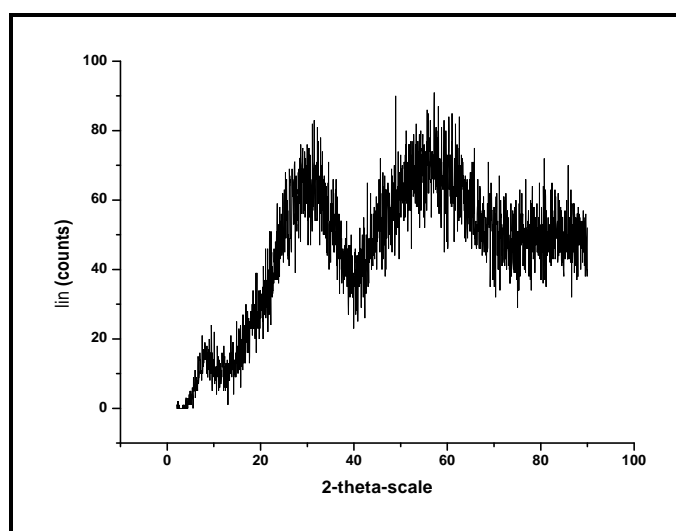


Figure 2.3 (c) XRD pattern of ZrPW

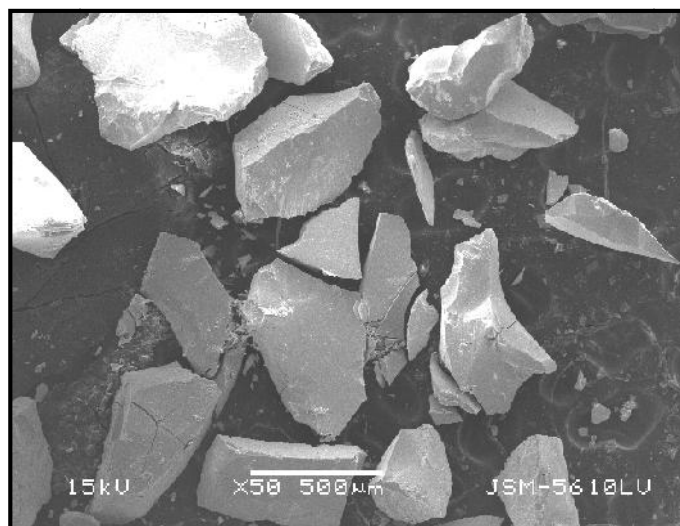


Figure 2.3 (d) SEM image of ZrPW

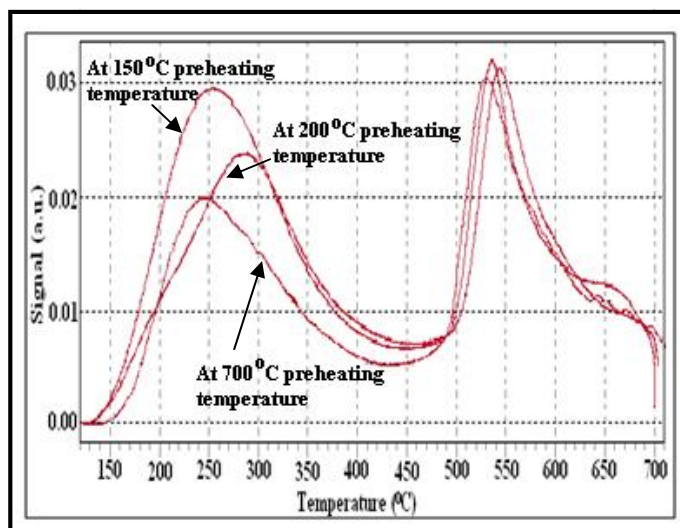


Figure 2.3 (e) NH₃-TPD patterns of ZrPW

Table 2.6 Characterization of TiPW

| Appearance | | White soft granules | | | |
|---|-----------------------------|--|-----------------------|------------------------|-----------------------|
| Cation exchange capacity (CEC)/Protonating ability | Temperature (°C) | CEC (meq.g ⁻¹) | | | |
| | RT | 3.48 | | | |
| | 150 | 2.97 | | | |
| | 200 | 2.39 | | | |
| Chemical Stability (Maximum tolerable limits) | Acids | 18N H ₂ SO ₄ , 16N HNO ₃ , 11.3N HCl | | | |
| | Bases | 5 N NaOH, 5 N KOH | | | |
| | Organic reagents | Ethanol, propanol, butanol, benzyl alcohol, 2-ethyl-1-hexanol, acetone, cyclohexane, toluene, xylene, benzyl chloride, acetyl chloride, anisole, veratrole, methyl acetoacetate, acetic acid benzaldehyde, cyclohexanone, acetophenone and nitrobenzene. | | | |
| Instrumental Methods of Analysis | | | | | |
| Elemental Analysis | Technique/Method | Elements | | | |
| | | Ti | P | W | |
| | ICP-AES (%) | 14.84 | 4.64 | 24.97 | |
| FTIR | Peaks (cm ⁻¹) | ~3400 cm ⁻¹ | ~1635cm ⁻¹ | ~1083 cm ⁻¹ | ~525 cm ⁻¹ |
| | Groups assigned | O-H _{str} | H-O-H _{ben} | P=O _{str} | W-O-P _{str} |
| TGA | Temperature range (°C) | 40-150 | | | |
| | % Weight loss | 21.02% (loss of surface moisture) | | | |
| | Temperature range (°C) | 150-650 | | | |
| | % Weight loss | 4.28 % (condensation of pendant -OH groups) | | | |
| XRD | Nature of material | Amorphous | | | |
| SEM | Size of particles | Irregular | | | |
| Catalyst characterization | | | | | |
| Surface area (by BET method) | | 86.48 m ² /g | | | |
| Average Pore diameter (nm) | | 10.17 | | | |
| Pore Volume (mL·g⁻¹) | | 0.21 | | | |
| Surface acidity (by NH₃-TPD method) | Preheating temperature (°C) | | Acidity (mmol/g) | | |
| | 150°C | | 11.05 | | |
| | 200°C | | 11.02 | | |
| | 700°C | | 8.28 | | |

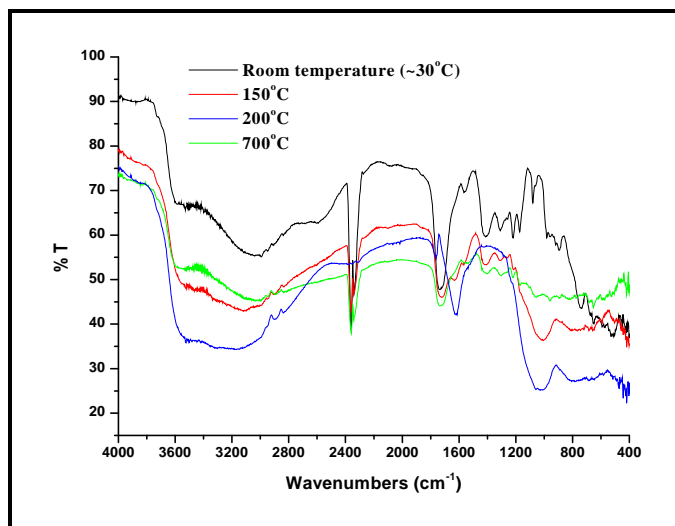


Figure 2.4 (a) FTIR spectra of TiPW

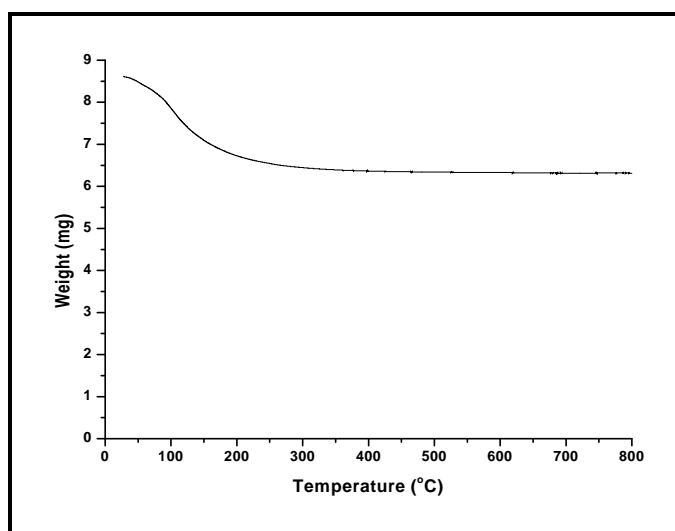


Figure 2.4 (b) TGA plot of TiPW

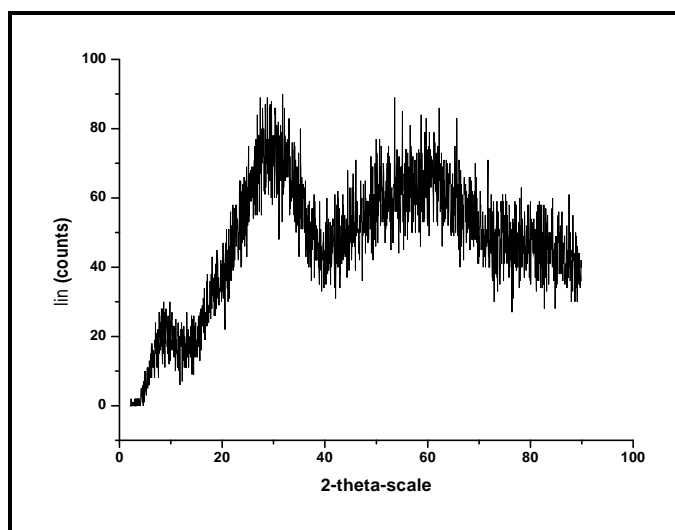


Figure 2.4 (c) XRD pattern of TiPW

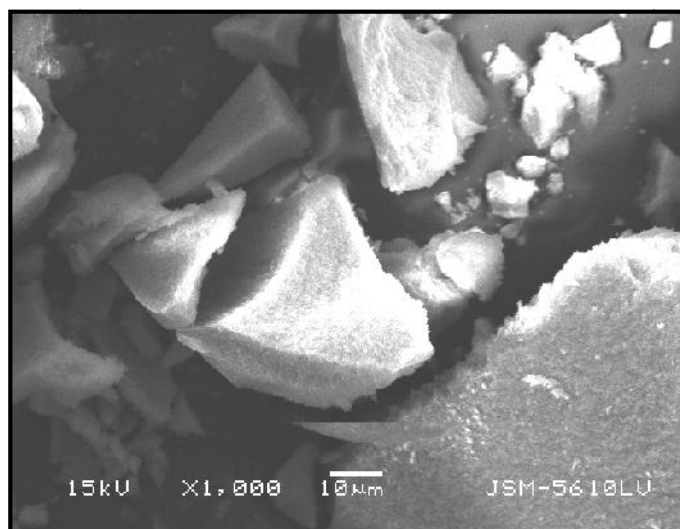


Figure 2.4 (d) SEM image of TiPW

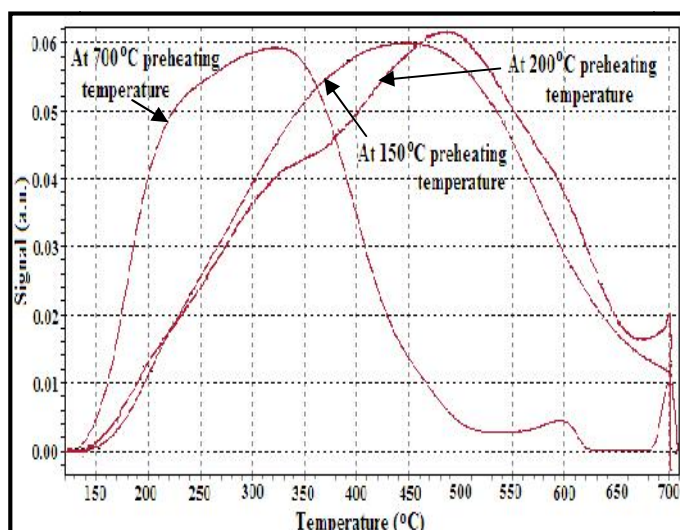


Figure 2.4 (e) NH₃-TPD patterns of TiPW

Table 2.7 Characterization of SnPW

| Appearance | | White hard granules | | | |
|---|-----------------------------|--|-----------------------|------------------------|-----------------------|
| Cation exchange capacity (CEC)/Protonating ability | Temperature (°C) | CEC (meq.g ⁻¹) | | | |
| | RT | 2.44 | | | |
| | 150 | 2.00 | | | |
| | 200 | 1.64 | | | |
| Chemical Stability (Maximum tolerable limits) | Acids | 18N H ₂ SO ₄ , 16N HNO ₃ , 11.3N HCl | | | |
| | Bases | 5 N NaOH, 5 N KOH | | | |
| | Organic reagents | Ethanol, propanol, butanol, benzyl alcohol, 2-ethyl-1-hexanol, acetone, cyclohexane, toluene, xylene, benzyl chloride, acetyl chloride, anisole, veratrole, methyl acetoacetate, acetic acid benzaldehyde, cyclohexanone, acetophenone and nitrobenzene. | | | |
| Instrumental Methods of Analysis | | | | | |
| Elemental Analysis | Technique/Method | Elements | | | |
| | | Sn | P | W | |
| | ICP-AES (%) | 36.82 | 4.67 | 29.41 | |
| FTIR | Peaks (cm ⁻¹) | ~3400 cm ⁻¹ | ~1635cm ⁻¹ | ~1083 cm ⁻¹ | ~525 cm ⁻¹ |
| | Groups assigned | O-H _{str} | H-O-H _{ben} | P=O _{str} | W-O-P _{str} |
| TGA | Temperature range (°C) | 40-150 | | | |
| | % Weight loss | 15.26 % (loss of surface moisture) | | | |
| | Temperature range (°C) | 150-650 | | | |
| | % Weight loss | 6.04 % (condensation of pendant -OH groups) | | | |
| XRD | Nature of material | Amorphous | | | |
| SEM | Size of particles | Irregular | | | |
| Catalyst characterization | | | | | |
| Surface area (by BET method) | | 171.04 m ² /g | | | |
| Average Pore diameter (nm) | | 1.88 | | | |
| Pore Volume (mL·g⁻¹) | | 0.08 | | | |
| Surface acidity (by NH₃-TPD method) | Preheating temperature (°C) | | Acidity (mmol/g) | | |
| | 150°C | | 10.28 | | |
| | 200°C | | 7.54 | | |
| | 700°C | | 4.50 | | |

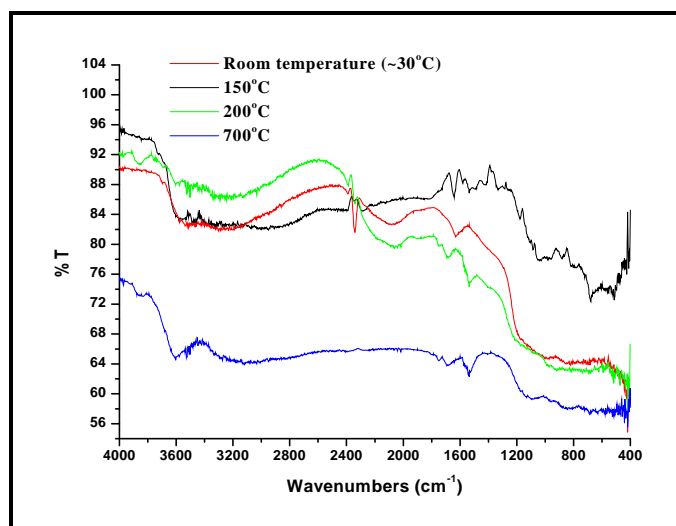


Figure 2.5 (a) FTIR spectra of SnPW

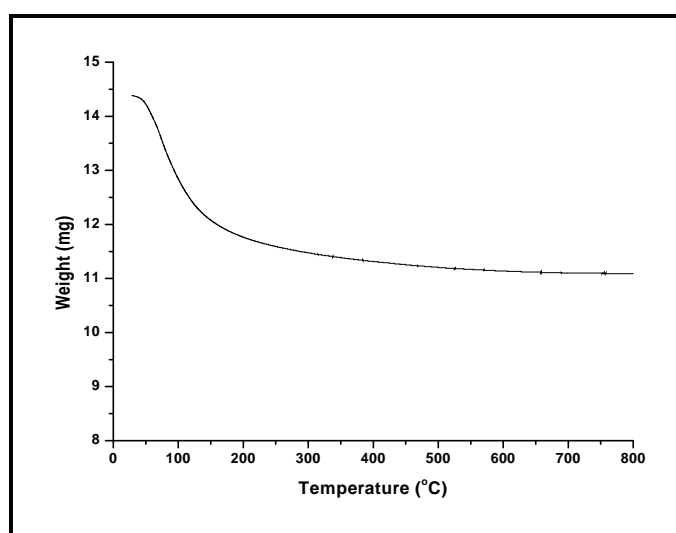


Figure 2.5 (b) TGA plot of SnPW

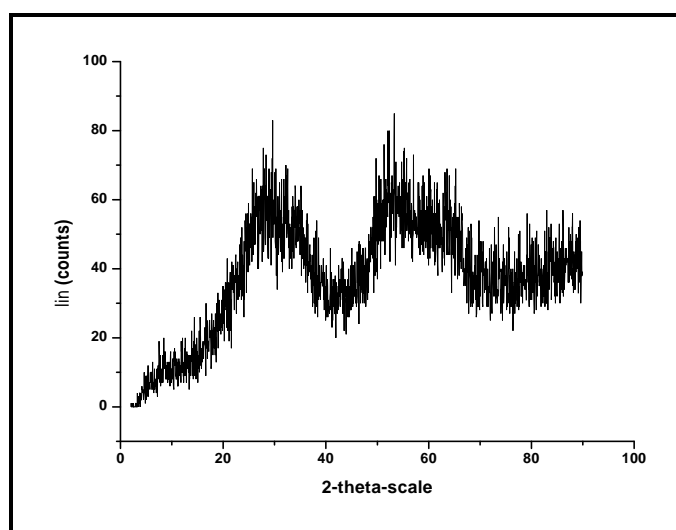


Figure 2.5 (c) XRD pattern of SnPW

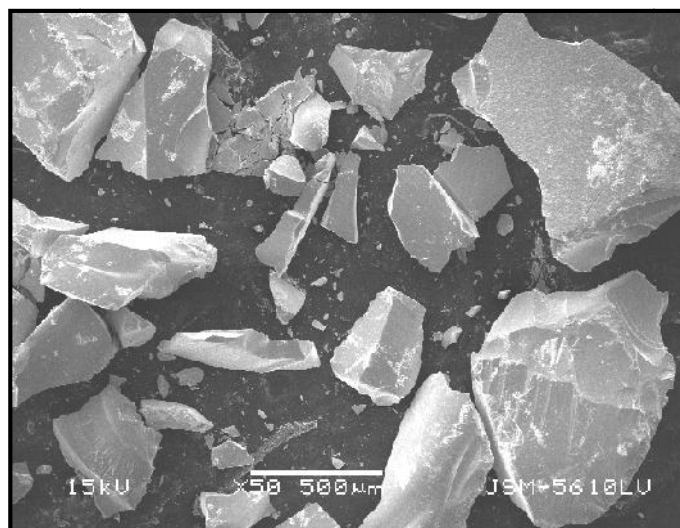


Figure 2.5 (d) SEM image of SnPW

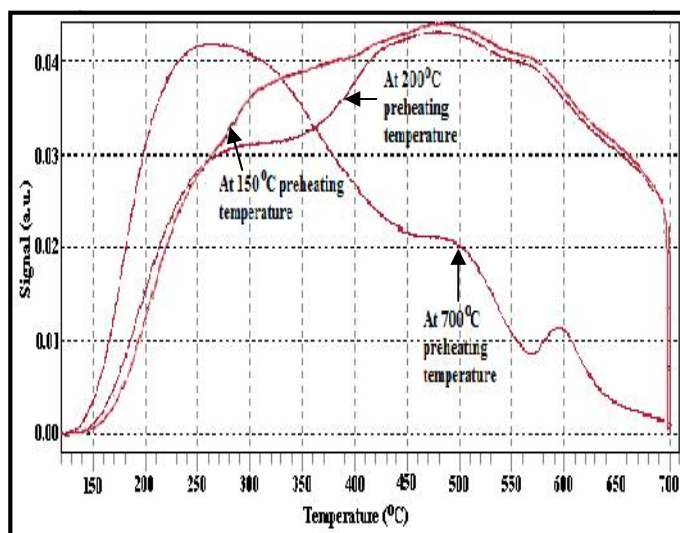


Figure 2.5 (e) NH₃-TPD patterns of SnPW

Table 2.8 Characterization of 12-TPA/ZrO₂-20

| Appearance | | White powder | | | |
|--|---------------------------|--|-----------------------|------------------------|-----------------------|
| Chemical Stability (Maximum tolerable limits) | Acids | 5N H ₂ SO ₄ , 16N HNO ₃ , 11.3N HCl | | | |
| | Bases | Not Stable | | | |
| | Organic reagents | Ethanol, propanol, butanol, benzyl alcohol, 2-ethyl-1-hexanol, acetone, cyclohexane, toluene, xylene, benzyl chloride, acetyl chloride, anisole, veratrole, methyl acetoacetate, acetic acid benzaldehyde, cyclohexanone, acetophenone and nitrobenzene. | | | |
| Instrumental Methods of Analysis | | | | | |
| Elemental Analysis | Technique/Method | Elements | | | |
| | | Zr | P | W | |
| | ICP-AES (%) | 58.62 | 0.09 | 16.48 | |
| FTIR | Peaks (cm ⁻¹) | ~3450 cm ⁻¹ | ~1635cm ⁻¹ | ~1083 cm ⁻¹ | ~987 cm ⁻¹ |
| | Groups assigned | O-H _{str} | H-O-H _{ben} | P=O _{str} | W-O _{str} |
| TGA | Temperature range (°C) | 30-150 | | | |
| | % Weight loss | 0.9 % (loss of surface moisture) | | | |
| XRD | Nature of material | Crystalline (JCPDS data card no. 17-923) | | | |
| SEM | Size of particles | Irregular | | | |
| Catalyst characterization | | | | | |
| Surface area (by BET method) | | 33.90 m ² /g | | | |
| Average Pore diameter (nm) | | 2.18 | | | |
| Pore Volume (mL·g⁻¹) | | 0.001 | | | |
| Surface acidity (by NH₃-TPD method) | | Preheating temperature (°C) | | Acidity (mmol/g) | |
| | | 150°C | | 1.07 | |
| | | 200°C | | 0.89 | |
| | | 700°C | | 0.17 | |

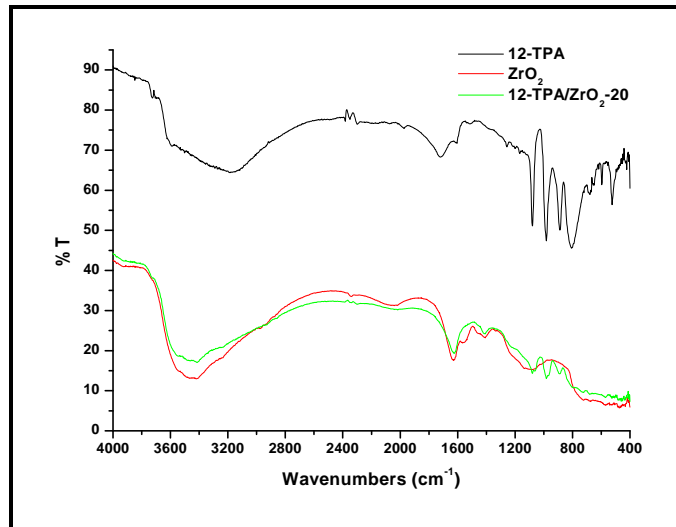


Figure 2.6 (a) FTIR spectra of 12-TPA/ZrO₂-20

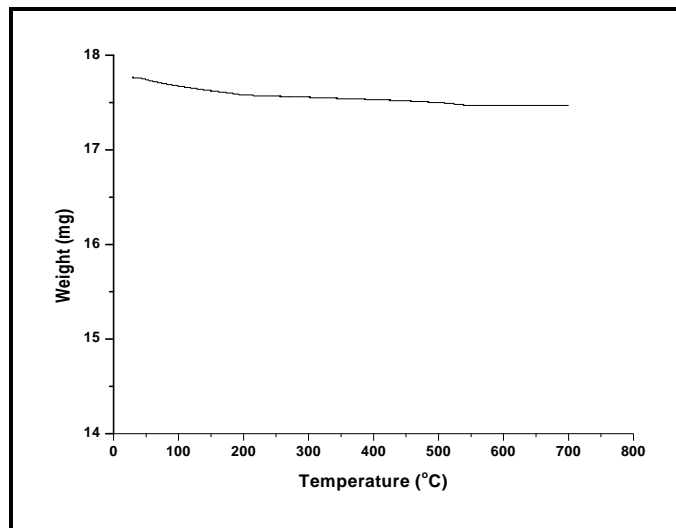


Figure 2.6 (b) TGA plot of 12-TPA/ZrO₂-20

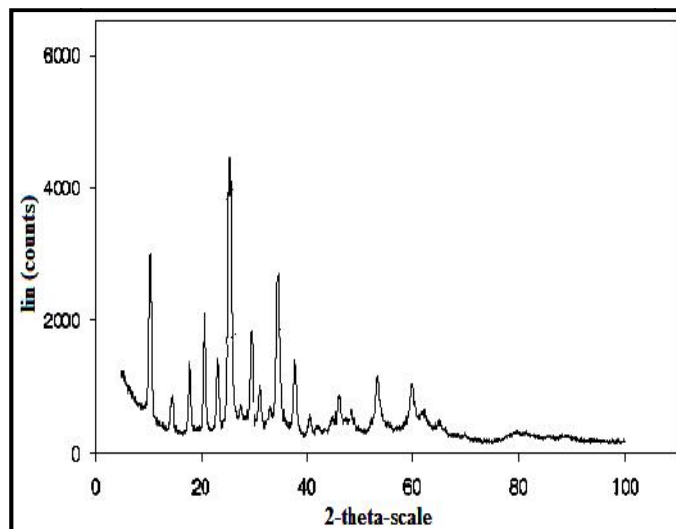


Figure 2.6 (c) XRD pattern of 12-TPA

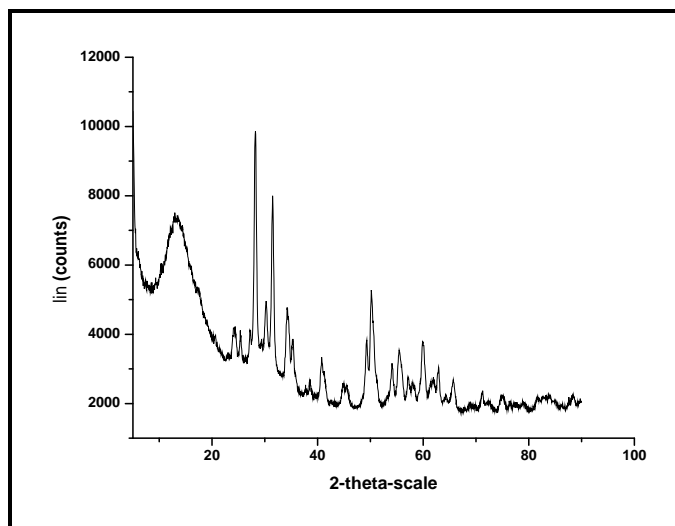


Figure 2.6 (d) XRD pattern of 12-TPA/ZrO₂-20

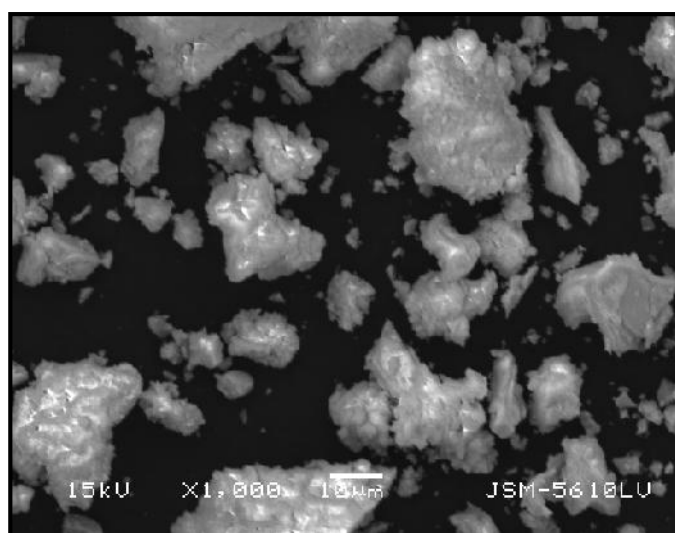


Figure 2.6 (e) SEM image of ZrO₂

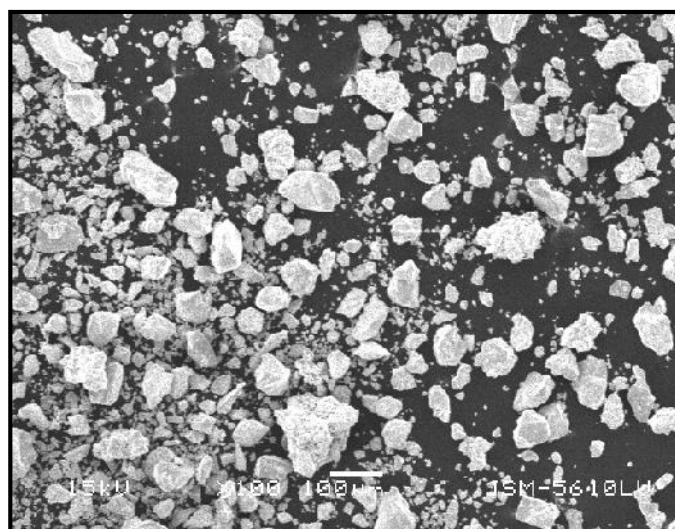


Figure 2.6 (f) SEM image of 12-TPA/ZrO₂-20

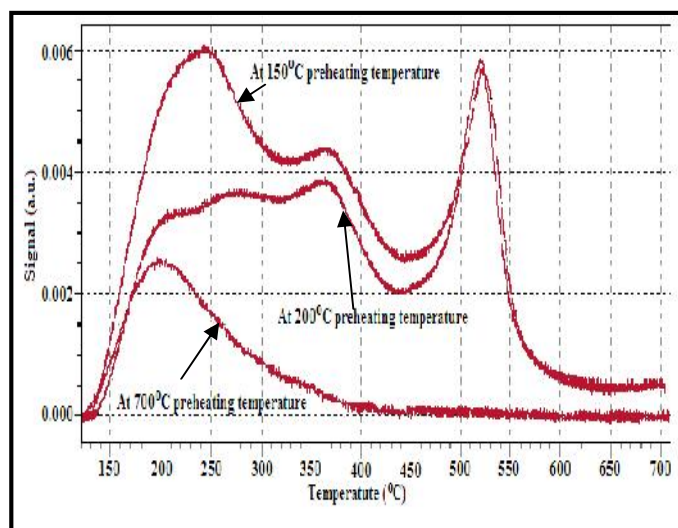


Figure 2.6 (g) NH₃-TPD patterns of 12-TPA/ZrO₂-20 .

Table 2.9 Characterization of 12-TPA/TiO₂-20

| Appearance | | White powder | | | |
|--|-----------------------------|--|-----------------------|------------------------|-----------------------|
| Chemical Stability (Maximum tolerable limits) | Acids | 5N H ₂ SO ₄ , 16N HNO ₃ , 11.3N HCl | | | |
| | Bases | Not Stable | | | |
| | Organic reagents | Ethanol, propanol, butanol, benzyl alcohol, 2-ethyl-1-hexanol, acetone, cyclohexane, toluene, xylene, benzyl chloride, acetyl chloride, anisole, veratrole, methyl acetoacetate, acetic acid benzaldehyde, cyclohexanone, acetophenone and nitrobenzene. | | | |
| Instrumental Methods of Analysis | | | | | |
| Elemental Analysis | Technique/Method | | Elements | | |
| | | | Ti | P | W |
| | ICP-AES (%) | | 48.76 | 0.08 | 16.17 |
| FTIR | Peaks (cm ⁻¹) | ~3450 cm ⁻¹ | ~1635cm ⁻¹ | ~1083 cm ⁻¹ | ~987 cm ⁻¹ |
| | Groups assigned | O-H _{str} | H-O-H _{ben} | P=O _{str} | W-O _{str} |
| TGA | Temperature range (°C) | 30-150 | | | |
| | % Weight loss | 0.4 % (loss of surface moisture) | | | |
| XRD | Nature of material | Crystalline (JCPDS data card no. 21-1272) | | | |
| SEM | Size of particles | Irregular | | | |
| Catalyst characterization | | | | | |
| Surface area (by BET method) | | 60.50 m ² /g | | | |
| Average Pore diameter (nm) | | 3.83 | | | |
| Pore Volume (mL·g⁻¹) | | 0.002 | | | |
| Surface acidity (by NH₃-TPD method) | Preheating temperature (°C) | | Acidity (mmol/g) | | |
| | 150°C | | 2.03 | | |
| | 200°C | | 1.68 | | |
| | 700°C | | 0.27 | | |

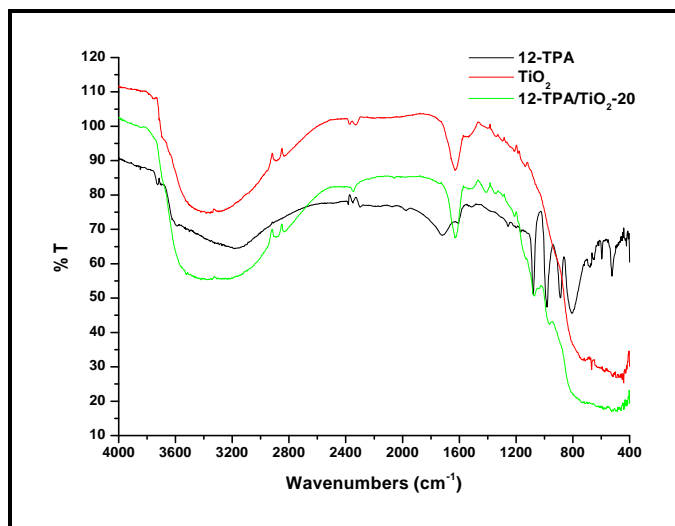


Figure 2.7 (a) FTIR spectra of 12-TPA/TiO₂-20

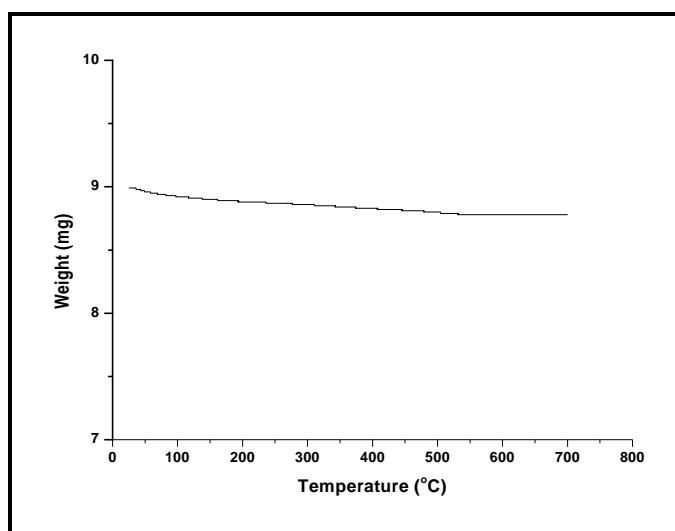


Figure 2.7 (b) TGA plot of 12-TPA/TiO₂-20

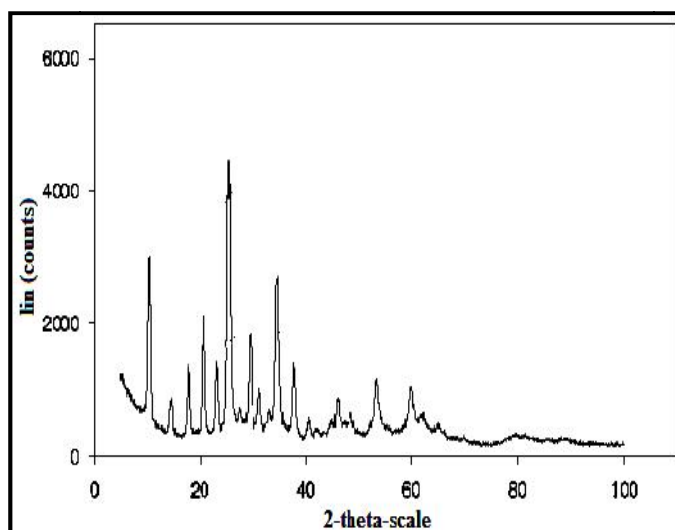


Figure 2.7 (c) XRD pattern of 12-TPA

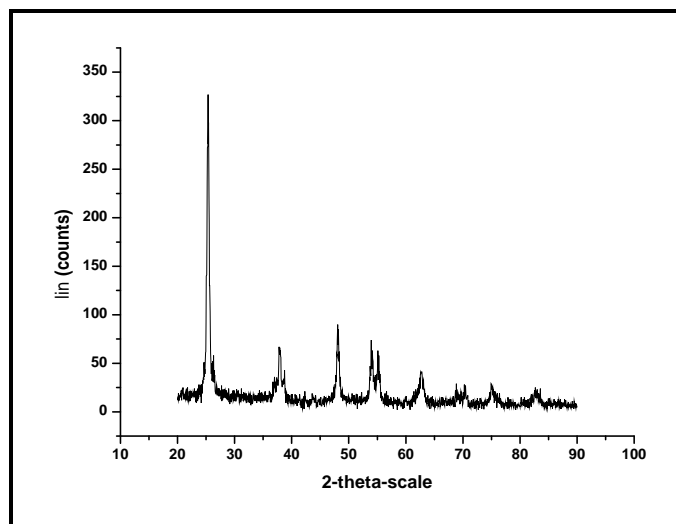


Figure 2.7 (d) XRD pattern of 12-TPA/TiO₂-20

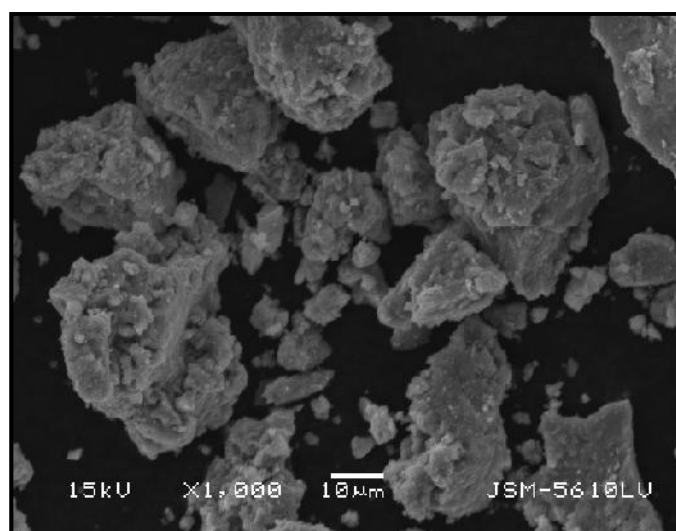


Figure 2.7 (e) SEM image of TiO₂

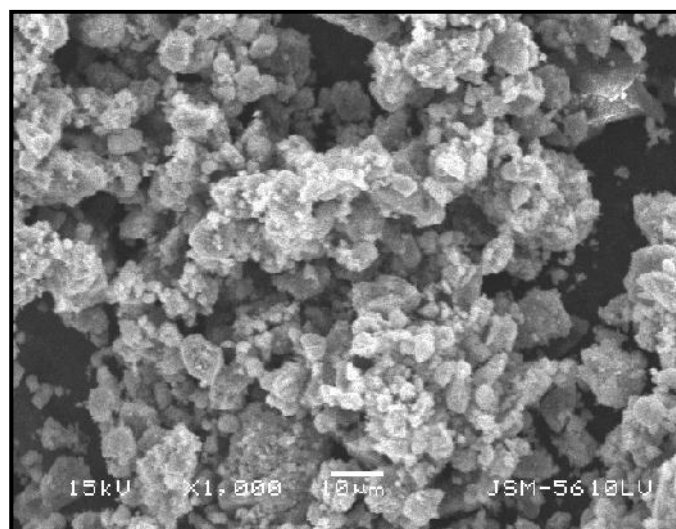


Figure 2.7 (f) SEM image of 12-TPA/TiO₂-20

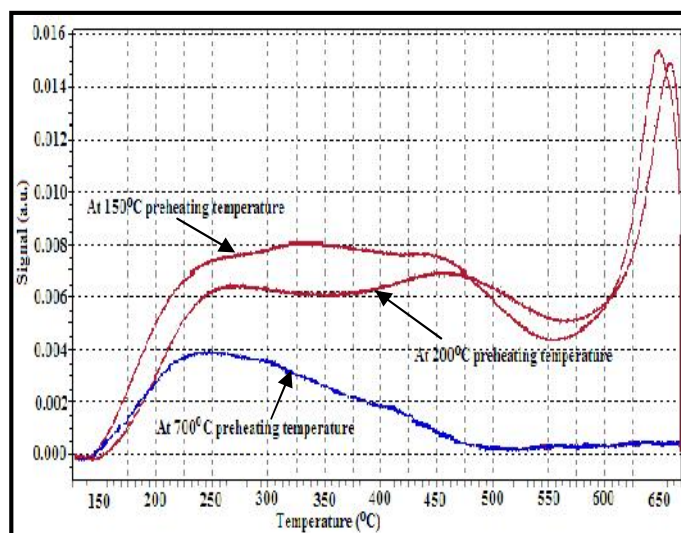


Figure 2.7 (g) NH₃-TPD patterns of 12-TPA/TiO₂-20 .

Table 2.10 Characterization of 12-TPA/SnO₂-20

| Appearance | | White powder | | | |
|--|---------------------------|--|-----------------------|------------------------|-----------------------|
| Chemical Stability (Maximum tolerable limits) | Acids | 5N H ₂ SO ₄ , 16N HNO ₃ , 11.3N HCl | | | |
| | Bases | Not Stable | | | |
| | Organic reagents | Ethanol, propanol, butanol, benzyl alcohol, 2-ethyl-1-hexanol, acetone, cyclohexane, toluene, xylene, benzyl chloride, acetyl chloride, anisole, veratrole, methyl acetoacetate, acetic acid benzaldehyde, cyclohexanone, acetophenone and nitrobenzene. | | | |
| Instrumental Methods of Analysis | | | | | |
| Elemental Analysis | Technique/Method | Elements | | | |
| | | Sn | P | W | |
| | ICP-AES (%) | 60.01 | 0.08 | 18.04 | |
| FTIR | Peaks (cm ⁻¹) | ~3450 cm ⁻¹ | ~1635cm ⁻¹ | ~1083 cm ⁻¹ | ~987 cm ⁻¹ |
| | Groups assigned | O-H _{str} | H-O-H _{ben} | P=O _{str} | W-O _{str} |
| TGA | Temperature range (°C) | 30-150 | | | |
| | % Weight loss | 1.4 % (loss of surface moisture) | | | |
| XRD | Nature of material | Crystalline (JCPDS data card no. 41-1445) | | | |
| SEM | Size of particles | Irregular | | | |
| Catalyst characterization | | | | | |
| Surface area (by BET method) | | 139.54 m ² /g | | | |
| Average Pore diameter (nm) | | 2.05 | | | |
| Pore Volume (mL·g⁻¹) | | 0.01 | | | |
| Surface acidity (by NH₃-TPD method) | | Preheating temperature (°C) | | Acidity (mmol/g) | |
| | | 150°C | | 1.42 | |
| | | 200°C | | 1.11 | |
| | | 700°C | | 0.22 | |

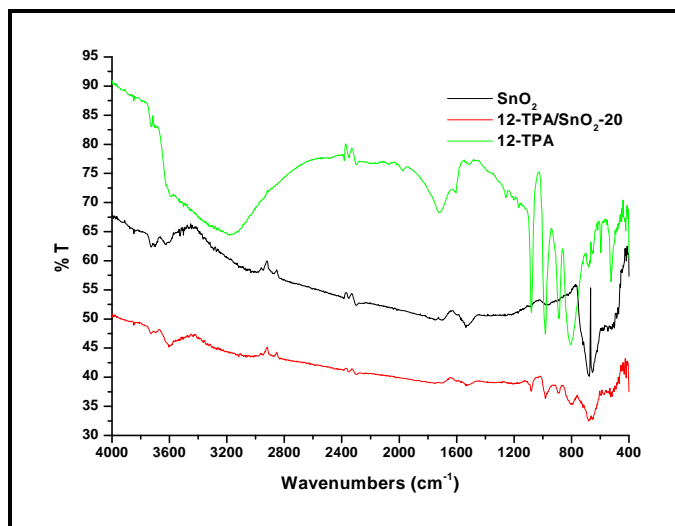


Figure 2.8 (a) FTIR spectra of 12-TPA/SnO₂-20

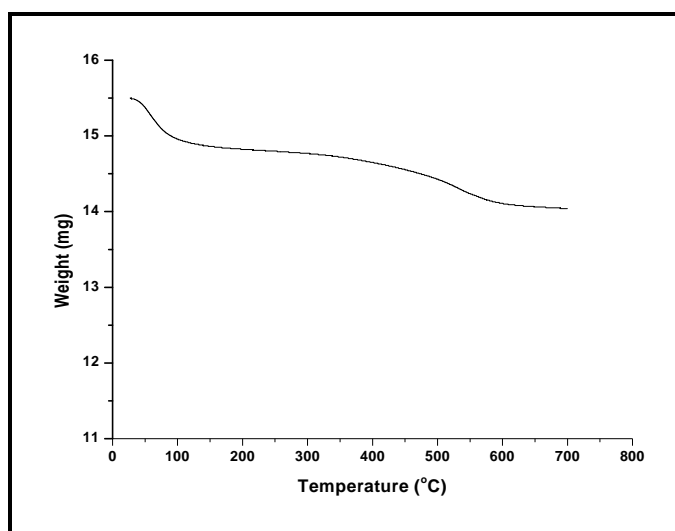


Figure 2.8 (b) TGA plot of 12-TPA/SnO₂-20

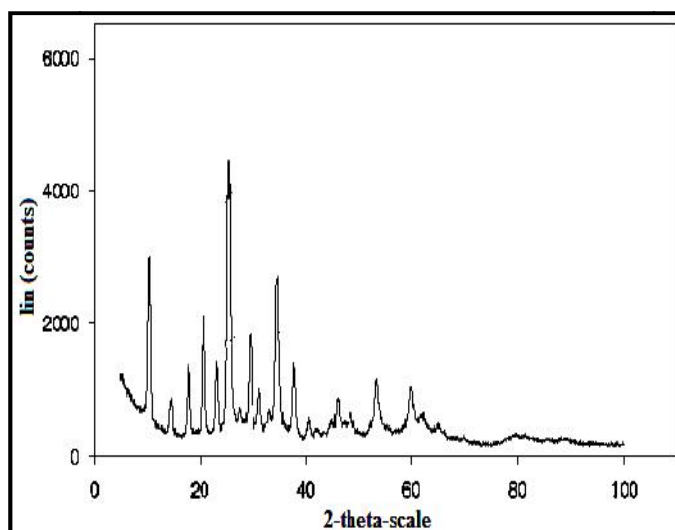


Figure 2.8 (c) XRD pattern of 12-TPA

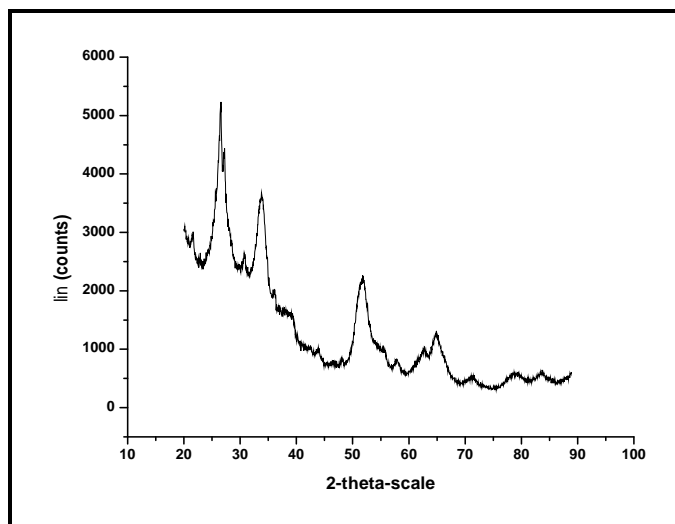


Figure 2.8 (d) XRD pattern of 12-TPA/SnO₂-20

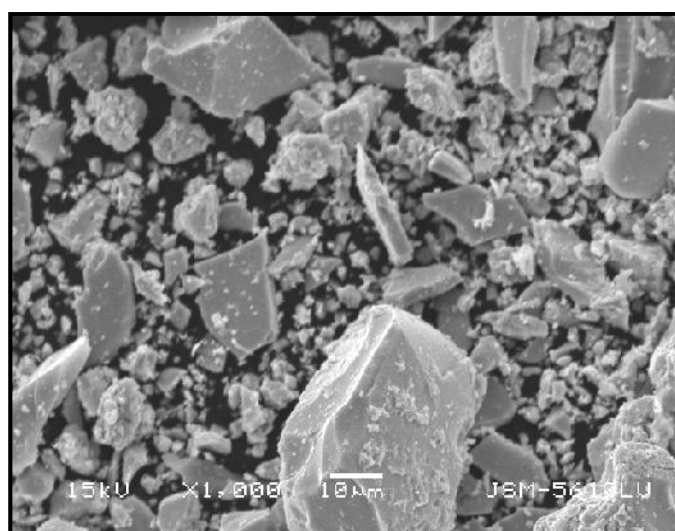


Figure 2.8 (e) SEM image of SnO₂

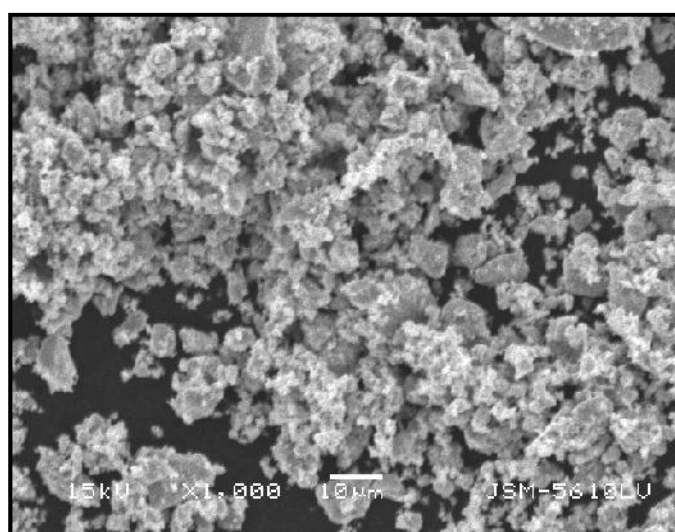


Figure 2.8 (f) SEM image of 12-TPA/SnO₂-20

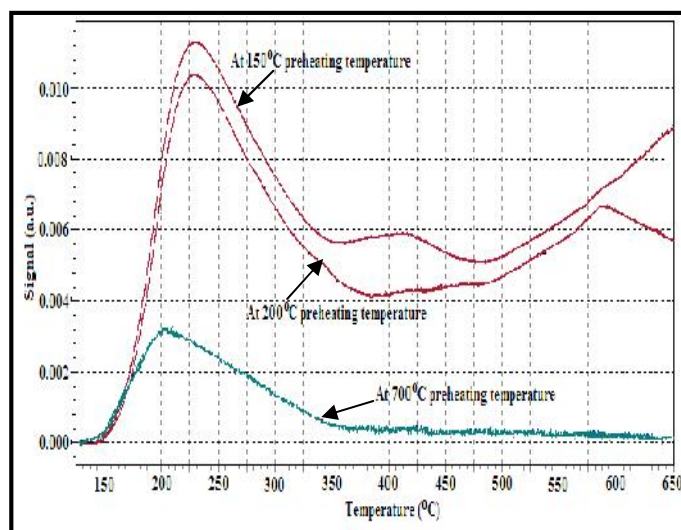


Figure 2.8 (g) NH₃-TPD patterns of 12-TPA/SnO₂-20 .

REFERENCES

1. Hiavacek V, Puszynski J, *Chemical engineering aspects of advanced ceramic materials*, Ind. Eng. Chem. Res. 35 (1996) 349-377.
2. Brinker C J, Scherer G W, *Sol-Gel Science: The Physics and Chemistry of Sol-Gel Processing*, Academic Press, Boston (1990).
3. Iler R K, *The Chemistry of Silica: Solubility, Polymerization, Colloid and Surface Properties, and Biochemistry*, John Wiley & Sons, New York (1979).
4. Davis P J, Brinker C J, Smith D M, Assink R A, *Pore structure evolution in silica gel during aging / drying: II. Effect of pore fluids*, J. Non-Cryst. Solids. 142 (1992)197-207.
5. Keshavaraja A, Ramaswamy V, Soni H S, Ramaswamy A V, Ratnasamy P, *Synthesis, Characterization, and Catalytic Properties of Micro-Mesoporous, Amorphous Titanosilicate Catalysts*, J. Catal. 157(2) (1995) 501-511.
6. Davis P J, Brinker C J, Smith D M, *Pore structure evolution in silica gel during aging/drying I. Temporal and thermal aging*, J. Non-Cryst. Solids. 142 (1992) 189-196.
7. Khder A S, *Preparation, characterization and catalytic activity of tin oxide-supported 12-tungstophosphoric acid as a solid catalyst*, Appl. Catal. A: Gen. 343(1-2) (2008) 109-116.
8. Bhaumik A, Inagaki S, *Mesoporous Titanium Phosphate Molecular Sieves with Ion-Exchange Capacity*, J Am. Chem. Soc. 123 (2001) 691-696.
9. Patel P, Chudasama U, *Synthesis and characterization of a novel hybrid cation exchange material and its application in metal ion separations*, Ion Exch. Lett. 4 (2011) 7-15.
10. Thakkar R, Chudasama U, *Synthesis and characterization of zirconium titanium phosphate and its application in separation of metal ions*, J. Haz. Mater. 172 (2009) 129-137.
11. Alberti G, Torracca E, *Crystalline insoluble acid salts of polyvalent metals and polybasic acids - VI: Preparation and ion-exchange properties of crystalline titanium arsenate*, J Inorg. Nucl. Chem. 30 (1968) 3075-3080.
12. Joshi R, Chudasama U, *Synthesis of coumarins via the Pechmann condensation using inorganic ion exchangers as solid acid catalysts*, J. Sci. Ind. Res. 67 (2008) 1092-1097.